

# Experimental and Theoretical Investigations of Magnetic Properties of Co Ferrite/Polyvinyl Alcohol Nanocomposites

S. Mirzaee<sup>1,2</sup> · S. Mahdaviifar<sup>3</sup> · S. Farjami Shayesteh<sup>3</sup>

Received: 8 November 2016 / Accepted: 12 May 2017 / Published online: 16 June 2017  
© Springer Science+Business Media New York 2017

**Abstract** Cobalt ferrite nanoparticles (NPs) have been synthesized by the modified co-precipitation technique in the presence of the polyvinyl alcohol (PVA) matrix. The structural and magnetic properties of NPs are tunable by means of interaction between the polymer and the surface of NPs. Magnetic properties of NPs were simulated using the accurate Monte Carlo (MC) method. In addition, the magnetic anisotropy constant has been obtained by means of the law of approach to saturation magnetization (LAS). The experimental and theoretical results are in good agreement with each other and show that the as-synthesized NPs are single domain and approximately non-interacting. The anisotropy constant and size of the NPs increase by increasing the concentration of precursors in the reaction medium. Nanocomposites have been characterized by X-ray diffraction (XRD) and Fourier transform infrared spectroscopy (FT-IR). Hysteresis loops were investigated at room temperature

using a vibrating sample magnetometer (VSM). The crystallite size of single-domain NPs is lower than 20 nm, and the obtained results from FT-IR confirmed the interaction between PVA and the surface of the particles. These approximately non-interacting NPs are useful for magnetic data storage.

**Keywords** Single domain particles · Co-ferrite · Polymer matrix · Coercivity

## 1 Introduction

Magnetic nanoparticles (NPs) are drawing increased attention, due to their unique physical properties and applications in diverse fields [1, 2]. Size, magnetization, and coercivity of the NPs play important roles in all of the applications like magnetic data storage. Increasing the bit density in data storage, especially in magnetic tape recording, depends strongly on the reduction of the MNPs' size. On the other hand, because of the superparamagnetic limit, the high magnetic anisotropy constant is necessary. Recent investigations about data storage device are focused on synthesizing the single-domain, non-interacting NPs with a high anisotropy constant [3, 4]. There are different methods for growing MNPs and control their properties, like co-precipitation in the presence of the polymer matrices [5] which is a relatively low-cost technique and has been extensively used to fabricate ferrites. Among all ferrimagnets, cobalt ferrite (NPs) shows unique properties such as strong magneto-crystalline anisotropy and great physical and chemical stability [6]. It also has an inverse spinel structure ( $AB_2O_4$ ) where the tetrahedral sites "A" are occupied by half of the Fe(III) ions and the octahedral sites "B" are occupied by the other half of the Fe ions together with Co(II) ions [7].

---

✉ S. Mirzaee  
s.mirzaee@uma.ac.ir

S. Mahdaviifar  
mahdaviifar@guilan.ac.ir

S. Farjami Shayesteh  
saber@guilan.ac.ir

<sup>1</sup> Department of Engineering Science, Faculty of Advanced Technologies, University of Mohaghegh Ardabili, Namin, Iran

<sup>2</sup> Department of Nanophysics, Faculty of Materials Engineering and Nanotechnology, Sabalan University of Advanced Technologies (SUAT), Namin, Iran

<sup>3</sup> Nanostructure Lab, Department of Physics, University of Guilan, P.O. Box. 1914, Rasht, Iran

Investigations about the different aspects of cobalt ferrite NPs have been made recently [8–12]. Coercivity, magnetization behavior versus temperature, as well as magneto-optical features and ion distribution have been considered in almost all of them. To the best of our knowledge, there is little investigation about the anisotropy constant or coercivity of  $\text{CoFe}_2\text{O}_4$  NPs especially in the presence of organic molecules like polymers which interact by the surface of NPs and effects of different concentrations of the precursor. Polyvinyl alcohol (PVA) is a water-soluble, nontoxic, and biocompatible polymer which is extensively used in different fields like foods and biomedical applications [13]. In this paper, PVA/  $\text{CoFe}_2\text{O}_4$  nanocomposites have been synthesized by the modified co-precipitation method. Different concentrations of metal ions are considered and allowed to interact with the polymer for hours. Magnetic properties of as-synthesized single-domain NPs are investigated experimentally. Also, the MC method has been used to simulate the magnetic properties. Also, the magnetic anisotropy constant was calculated by means of the LAS method. The obtained results from simulation and experiments are in good agreement with each other. The results show that the NPs are single domain and their magnetic properties are affected by the change of concentration of precursors and the intensity of interaction between PVA and the surface of the NPs.

## 2 Materials and Methods

All chemical materials were used as received, including iron chloride hexahydrate  $\text{FeCl}_3 \cdot 6\text{H}_2\text{O}$ , cobalt chloride hexahydrate ( $\text{CoCl}_2 \cdot 6\text{H}_2\text{O}$ ), and sodium hydroxide (NaOH) and PVA, which were purchased from the Merck Chemical Corporation.

Four samples with different concentrations of precursors were synthesized, as shown in Table 1. The  $\text{CoCl}_2$  and  $\text{FeCl}_3$  were stirred with PVA solution (25 ml 2%) at 75 °C for 7–10 min, and then left for 18 h; afterwards, NaOH was added to the mixture when its temperature released to 75 °C and the solution stirred for 1 h. All the dark brown samples dried after washing several times with deionized water, for 24 h at 60 °C.

**Table 1** Concentrations of precursors in the solution

| Samples | $\text{Co}^{2+}$ concentration | $\text{Fe}^{3+}$ concentration | NaOH concentration | Solution |
|---------|--------------------------------|--------------------------------|--------------------|----------|
| 1-a     | 0.1 M                          | 0.20 M                         | 2.00 M             | 75 ml    |
| 1-b     | 0.15 M                         | 0.30 M                         | 3.00 M             | 75 ml    |
| 1-c     | 0.20 M                         | 0.40 M                         | 4.00 M             | 75 ml    |
| 1-d     | 0.25 M                         | 0.50 M                         | 5.00 M             | 75 ml    |

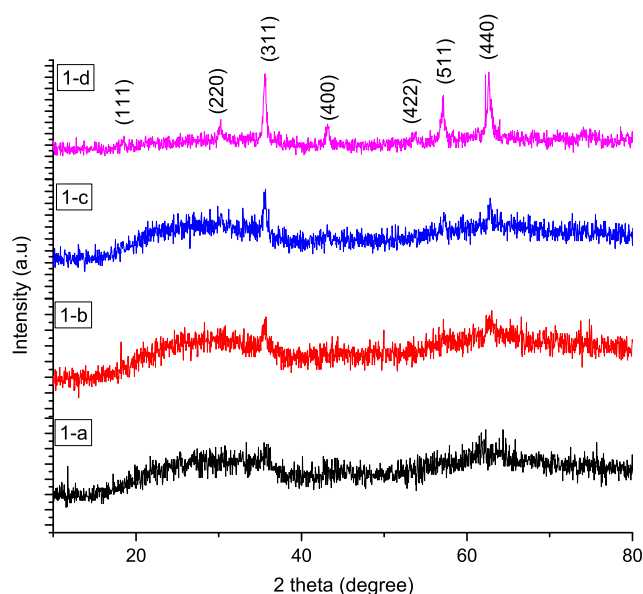


**Fig. 1** The XRD patterns of samples 1-a to d

### 2.1 MC Method

Considering a system containing non-interacting and single-domain magnetic particles which are substituted in an external magnetic field, the magnetic energy of such a system can be written as follows:

$$E_i = -K V_i (\hat{e}_i \cdot \hat{\mu}_i)^2 - \mu_i \cdot H \quad (1)$$

Where the first term is the magnetic anisotropy energy and the second is the Zeeman energy for  $i$ th particles [14]. For simplicity, the uniaxial type of anisotropy was chosen. In the first term,  $K$  is the effective anisotropy constant and  $V$  is the volume of the  $i$ th particle. In addition, the applied field is in the  $z$  direction. Supposing  $E_{\text{ini}}$  is the initial energy of nanoparticle  $i$  and  $E_{\text{fin}}$  is the energy of the final state, the probability of flipping the magnetic moment depends on the profile energy regarding the applied magnetic field. If  $h = H/H_k$  where  $H_k = 2K/M_s$  and  $M_s$  is the saturation magnetization, then two regions can be considered. The first is a region in which  $|h| > h_c(\alpha_i)$  and the second is a region in which  $|h| < h_c(\alpha_i)$ , where  $h_c(\alpha_i) =$

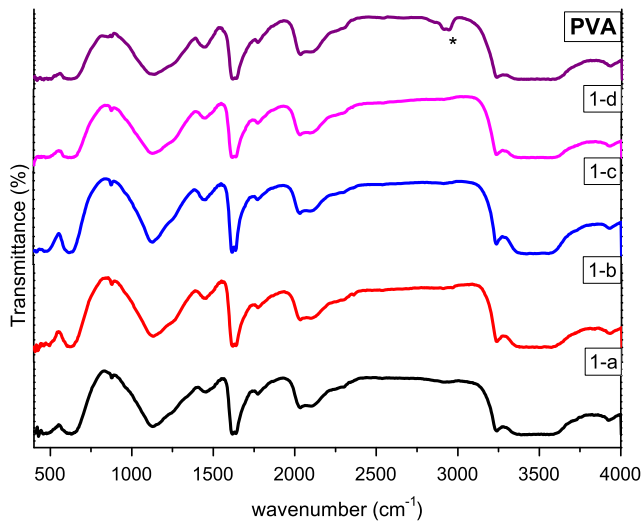


**Fig. 2** FT-IR spectra of PVA and samples 1-a to d in transmittance mode

$[(\sin\alpha_i)^{2/3} + (\cos\alpha_i)^{2/3}]^{-3/2}$ . In the first region, the probability of flipping the magnetization is calculated by  $p = \exp[-(E_{fin} - E_{ini})/k_B T]$  and in the other one, due to the existence of a saddle point, the probability can be written by  $p = \exp[-(E_{sad} - E_{ini})/k_B T]$  in which  $E_{sad}$  is the energy of the saddle point [15].

### 2.2 LAS Method

When a strong enough magnetic field applies to a magnetic material, the magnetization reaches the saturation amount where the magnetic field and magnetization vectors are approximately in the same direction. Hence, the magnetization can be written as

$$M = M_s \left( 1 - \frac{b}{H^2} - \dots \right) \tag{2}$$

where  $M_s$  is the saturation magnetization,  $H$  is the applied magnetic field,  $b$  can be written as  $\beta K_{eff}^2/M_s^2$  according to

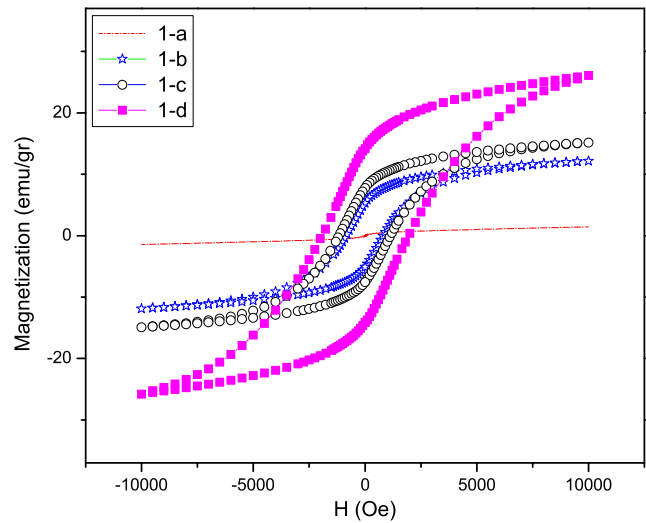


**Fig. 3** Hysteresis loops of samples 1-a to d obtained at room temperature

the anisotropy type, and  $\beta$  is a constant parameter which is 4/15 for uniaxial anisotropy. The experimental expression of the first derivative of LAS can be written as

$$\frac{dM}{dH} = M_s \left( \frac{a}{H^2} + \frac{2b}{H^3} + \dots \right) \tag{3}$$

where the first term is the stress field [16, 17].

### 3 Results

Figure 1 shows the XRD patterns of the as-synthesized samples. Samples 1-c and d have a cubic spinel structure and pure phase of  $\text{CoFe}_2\text{O}_4$  due to the diffraction peaks, which are well matched with the standard JCPDS card no. 22-1086, but the other samples have an approximately poor crystalline structure and peak intensity.

Scherrer’s formula [18],  $d = 0.9\lambda/(\beta \cos\theta)$ , is used for obtaining the average crystallite sizes of the samples, where

**Table 2** FT-IR absorption band for pure PVA and samples 1-a to d

|      | PVA  | 1-a  | 1-b  | 1-c  | 1-d  | Vibrational assignments    |
|------|------|------|------|------|------|----------------------------|
| –    | –    | 594  | 594  | 594  | 594  | Fe–O                       |
| 640  | 632  | 632  | 620  | 617  | 632  | CH <sub>2</sub> stretching |
| 1130 | 1131 | 1131 | 1133 | 1131 | 1130 | C–O                        |
| 1446 | 1457 | 1457 | 1454 | 1457 | 1454 | CH <sub>2</sub> bending    |
| 1620 | 1619 | 1619 | 1919 | 1619 | 1616 | $\delta(\text{H-O-H})$     |
| 2940 | –    | –    | –    | –    | –    | C–H stretching             |
| 3500 | 3239 | 3236 | 3236 | 3236 | 3236 | O–H bending                |
| 3930 | 3926 | 3930 | 3930 | 3930 | 3930 | O–H free stretching        |

**Table 3** Experimental and MC results obtained for samples 1-a to d

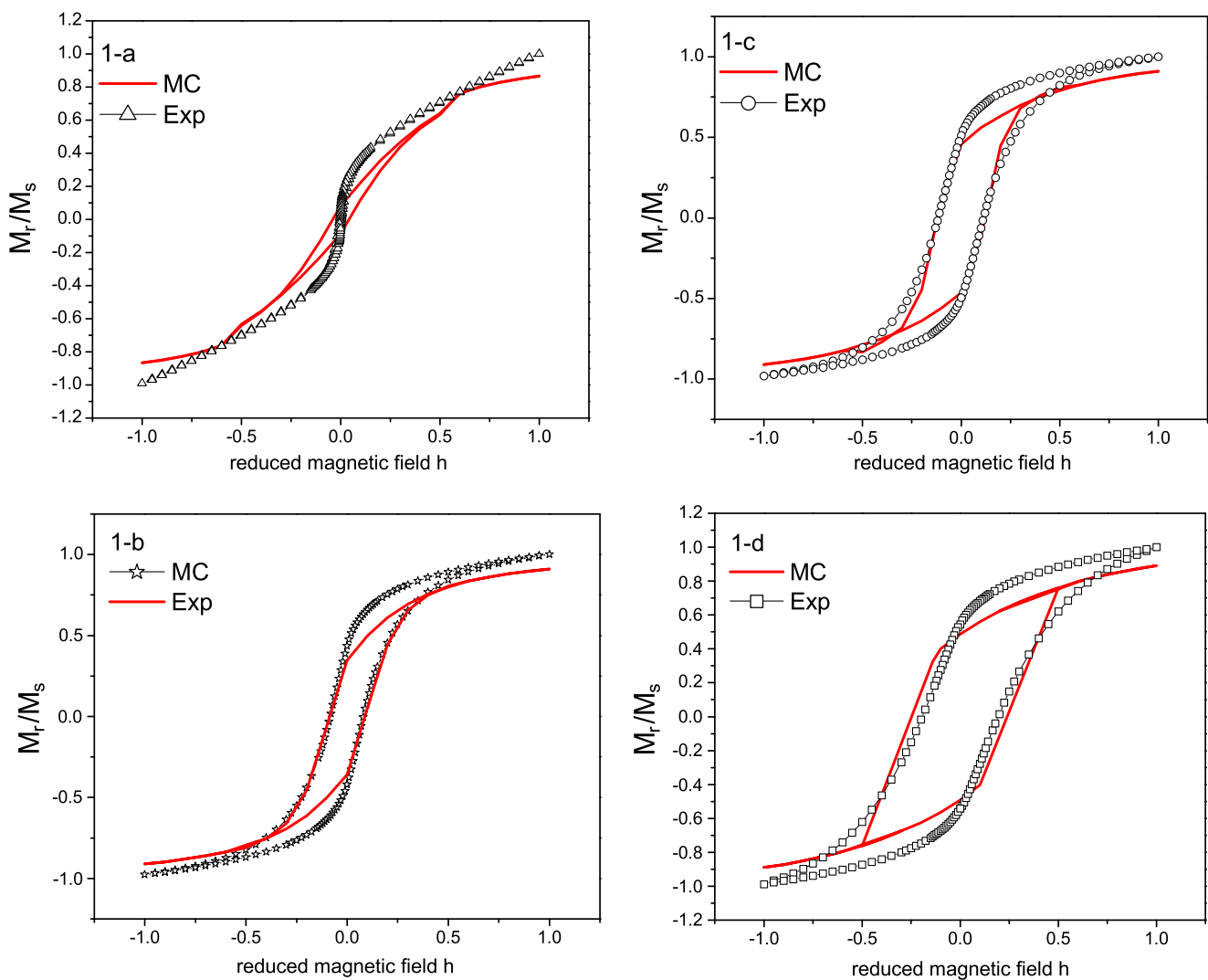
| Samples | $d_{\text{XRD}}$<br>(nm) | Saturation<br>magnetization<br>$M_s$ (emu/g) | Reduced<br>magnetization<br>$M_r/M_s$<br>EXP-MC | Coercivity<br>$H_c$ (Oe) | Anisotropy<br>constant<br>$K_{\text{eff}}(\text{MC})$<br>$\text{J/m}^3$ | Anisotropy<br>constant<br>$K_{\text{eff}}(\text{exp})$<br>$\text{J/m}^3$ |
|---------|--------------------------|--|---|--------------------------|---|--|
| 1-a     | 7                        | 1.42   | 0.00–0.10                                       | 0                        | –   | –  |
| 1-b     | 10                       | 12.15  | 0.43–0.34                                       | 800                      | $3 \times 10^4$   | $0.2 \times 10^4$  |
| 1-c     | 13                       | 15.19  | 0.51–0.45                                       | 1100                     | $2 \times 10^4$   | $0.3 \times 10^4$  |
| 1-d     | 17                       | 26.09  | 0.562–0.48                                      | 2000                     | $1 \times 10^5$   | $0.5 \times 10^4$  |

$\beta$  is the full width at half maxima of the strongest intensity diffraction peak (311),  $\lambda$  is the wavelength of radiation, and  $\theta$  is the angle of the strongest peak. Table 3 shows the crystallite sizes of the samples.

For identifying the interaction of the polymer by the surface of NPs in nanocomposites, the FT-IR analysis was

done. The obtained spectra of PVA and the other four samples are illustrated in Fig. 2.

In the spectrum of pure PVA, the absorption band observed at  $3930 \text{ cm}^{-1}$  is an alcoholic O–H stretching band. The dip obtained at  $2940 \text{ cm}^{-1}$  is attributed to C–H stretching vibration. The bonds located at  $1440$  and  $640 \text{ cm}^{-1}$

**Fig. 4** Experimental and simulated hysteresis loops of samples 1-a to d

are related to bending and stretching modes of the CH<sub>2</sub> group and C–O stretching vibration observed at 1130 cm<sup>-1</sup> [10]. The vibrations of ions in the crystal lattice usually appear in the range 100–1000 cm<sup>-1</sup>. In our samples, the intrinsic vibration of the tetrahedral sites of spinel ferrites is attributed to the bond at 580–600 cm<sup>-1</sup>. According to Table 2, the C–O absorption band in PVA shifts to a higher frequency in approximately all the samples, which means PVA interacted with the surface of magnetic NPs.

The hysteresis loops at room temperature are shown in Fig. 3. A magnetic field of 1.19 × 10<sup>6</sup> A/m (15 kOe) was applied. The magnetic properties are summarized in Table 3.

The simulated hysteresis loops of samples 1-a to d at room temperature have been shown in Fig. 4. For obtaining the anisotropy constant by means of the LAS method, according to Eq. 3, *b* parameter obtains from *dM/dH* vs

1/*H*<sup>3</sup> curve. Figure 5 illustrates the aforementioned curves for samples 1-c, b, and d and the linear fitting.

### 4 Discussion

According to Fig. 1, when the concentration of the precursors increase in the reaction medium, the crystal structure becomes perfect due to better ion diffusion in the solution. This may result in the favorable distribution of ions in the tetrahedral and octahedral sites. So, the XRD peaks get sharper and the size of the nanoparticles gets bigger. It is known that the magnetization reversal in magnetic particles occurs in different ways with respect to their size. For a better comparison, the coercivity versus particle size for magnetic particles and our nanocomposites are shown in Fig. 6.

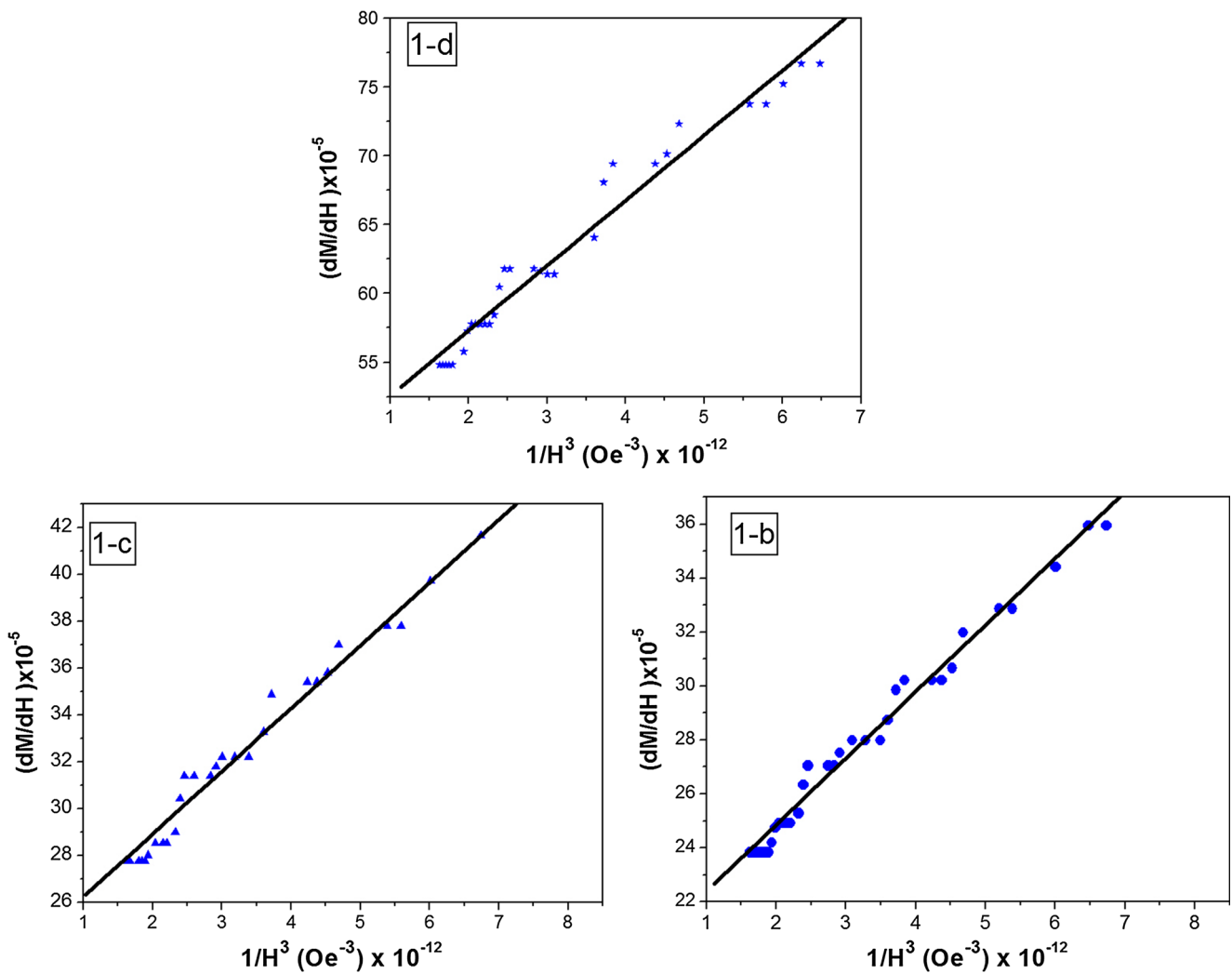
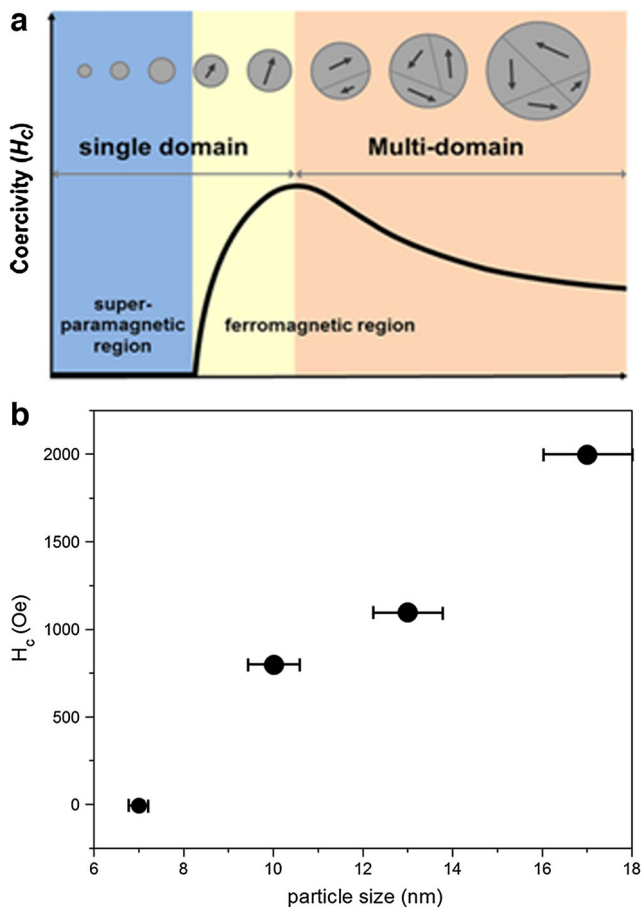


Fig. 5 The *dM/dH* vs 1/*H*<sup>3</sup> and linear fitting of samples 1-c, b, and d



**Fig. 6** Coercive field vs. particle size (a) [21] and for nanocomposites 1-a to d (b)

It is clear that the as-synthesized nanocomposites contain the nanoparticles which are in the single-domain region. Considering Table 2 and Fig. 2, the absorption band in  $1130\text{ cm}^{-1}$  (C–O) shifts to the higher wavenumber for samples 1-a, 1-b, and 1-c which means the polymer interacts by the surface of the NPs. But it does not change in sample 1-d. It is related to the high concentration of precursors in the reaction medium which causes the growth of nanoparticles out of the polymer matrix.

Table 3 and Fig. 4 show that the obtained results from MC simulation and experimental hysteresis loops are in good agreement with each other and the magnetic energy that has been assumed in MC simulation demonstrates the physics of the as-synthesized nanocomposites. The uniaxial anisotropy has been chosen as the magnetic anisotropy energy while a nuance exists in reduced magnetization. It can be related to this fact that the cubic anisotropy still participates in the magnetic energy of the system.

The surface effect, distribution of metal ions in spinel structures, size, and size distribution of magnetic NPs are some of the factors that have important effects on magnetic properties of NPs. As can be seen in Table 3, the obtained

coercivity and anisotropy constant from MC and LAS methods are smaller than the reported amounts for bare cobalt ferrite NPs [19]. When the NPs are covered by an organic shell or incorporated to the organic matrix like polymer, the molecules of the matrix occupy the vacancy on the surface, then the anisotropy decreases [20]. In our case, when the concentrations of the precursors increase, it causes the NPs' growth mostly out of the matrix and the interaction between the polymer and the surface of NPs decreases. So, it is expected that sample 1-d has a greater coercivity relative to the other samples. These single-domain NPs with tunable coercivity are useful for magnetic data storage and hyperthermia.

## 5 Conclusion

We have shown that by the simple corrected co-precipitation method, cobalt ferrite NPs can be synthesized in PVA matrix in a single-domain region. On the other hand, the assumptions in MC simulation confirmed the experimental results. Uniaxial anisotropy is the dominant type that exists in nanocomposites, and the PVA matrix attached to the surface of NPs reduced their anisotropy constant.

## References

- Liu, J., Qia, S.Z., Hu, Q.H., Lu, G.Q.: Magnetic nanocomposites with mesoporous structures: synthesis and applications. *Small* **4**, 425–443 (2011)
- Li, X.M., Liu, H.L., Fang, N., Wang, X.H., Wu, J.H.: Synthesis of bi-phase dispersible core-shell FeAu@ZnO magneto-optofluorescent nanoparticles. *Sci. Rep.* **5**, 16384–16394 (2015)
- Dai, Q., Berman, D., Virwani, K., Frommer, J., Jubert, P.O., Lam, M., Topuria, T., Imano, W., Nelson, A.: Self-assembled ferrimagnet polymer-composites for magnetic recording media. *Nano Lett.* **10**, 3216–3221 (2010)
- Fantechi, E., Campo, G., Carta, D., Corrias, A., de Julián Fernandez, C., Gatteschi, D., Innocenti, C., Pineider, F., Rugi, F., Sangregorio, C.: Exploring the effect of Co doping in fine maghemite nanoparticles. *J. Phys. Chem. C* **116**, 8261–8270 (2012)
- García-Cerda, L.A., Escaren o-Castro, M.U., Salazar-Zertuche, M.: Preparation and characterization of polyvinyl alcohol-cobalt ferrite nanocomposites. *J. Non-Cryst. Solids* **353**, 808–810 (2007)
- Jiang, J., Ai, L.H., Liu, A.H.: A novel poly(o-anisidine)/CoFe<sub>2</sub>O<sub>4</sub> multifunctional nanocomposite: preparation, characterization and properties. *Syn. Met.* **160**, 333–336 (2010)
- Naseri, M.G., Saion, E.B., Ahangar, H.A., Hashim, M., Shaari, A.H.: Simple preparation and characterization of nickel ferrite nanocrystals by a thermal treatment method. *Powder Technol.* **212**, 80–88 (2011)
- Sohn, H., Victora, R.H.: Optimization of magnetic anisotropy and applied fields for hyperthermia applications. *J. Appl. Phys.* **107**, 09B312-3 (2010)
- López, D., Cendoya, I., Torres, F., Tejada, J., Mijangos, C.: Preparation and characterization of poly(vinyl alcohol)-based magnetic

- nanocomposites. I. Thermal and mechanical properties. *J. Appl. Polym. Sci.* **82**, 3215–3222 (2001)
10. Salunkhe, A.B., Khot, V.M., Thorat, N.D., Phadatare, M.R., Sathish, C.I., Dhawale, D.S., Pawar, S.H.: Polyvinyl alcohol functionalized cobalt ferrite nanoparticles for biomedical applications. *Appl. Surf. Sci.* **264**, 598–604 (2013)
  11. Choueikani, F., Royer, F., Jamon, D., Siblini, A., Rousseau, J.J., Neveu, S., Charara, J.: Magneto-optical waveguides made of cobalt ferrite nanoparticles embedded in silica/zirconia organic-inorganic matrix. *Appl. Phys. Lett.* **94**, 051113-6 (2009)
  12. Venturelli, L., Nappini, S., Bulfoni, M., Gianfrancesch, G., Zilio, S.D., Coceano, G., Del Ben, F., Turetta, M., Scoles, G., Vaccari, L., Cesselli, D., Cojoc, D.: Glucose is a key driver for GLUT1-mediated nanoparticles internalization in breast cancer cells. *Sci. Rep.* **6**, 21629–21643 (2016)
  13. Kayal, S., Ramanujan, R.V.: Doxorubicin loaded PVA coated iron oxide nanoparticles for targeted drug delivery. *Mater. Sci. Eng. C* **30**, 484–490 (2010)
  14. Xu, C., Li, Z.Y., Hui, P.M.: Monte Carlo studies of hysteresis curves in magnetic composites with fine magnetic particles. *J. Appl. Phys.* **89**, 3403–3407 (2001)
  15. Du, H.F., Du, A.: Characterizing the magnetic anisotropy constant of spinel cobalt ferrite nanoparticles. *J. Appl. Phys.* **99**, 104306-14 (2006)
  16. Chikazumi, S.: *Physics of Ferromagnetism*. Oxford University Press, Oxford (1997)
  17. Herbst, J.F., Pinkerton, F.E.: Law of approach to saturation for polycrystalline ferromagnets: remanent initial state. *Phys. Rev. B* **57**, 10733 (1998)
  18. Cullity, B.D., Stock, S.R.: *Elements of X Ray Diffraction*. Addison Wesley, Boston (2001)
  19. Rondinone, A.J., Samia, A.C.S., Zhang, Z.J.: Characterizing the magnetic anisotropy constant of spinel cobalt ferrite nanoparticles. *Appl. Phys. Lett.* **76**, 3624–36246 (2000)
  20. Peddis, D., Orrù, F., Ardu, A., Cannas, C., Musinu, A., Piccaluga, G.: Interparticle interactions and magnetic anisotropy in cobalt ferrite nanoparticles. *Influ. Mol. Coat. Chem. Mater.* **24**, 1062–1071 (2012)
  21. Lee, J.S., Cha, J.M., Yoon, H.Y., Lee, J.K., Kim, Y.K.: Magnetic multi-granule nanoclusters: a model system that exhibits universal size effect of magnetic coercivity. *Sci. Rep.* **5**, 12135–12142 (2015)